PROCEEDINGS OF SPIE

SPIEDigitalLibrary.org/conference-proceedings-of-spie

Multipolar scattering analysis of a hybrid metal-dielectric stacked nanoantenna

Kiselev, Andrei, Ray, Debdatta, Martin, Olivier J.

Andrei Kiselev, Debdatta Ray, Olivier J. F. Martin, "Multipolar scattering analysis of a hybrid metal-dielectric stacked nanoantenna," Proc. SPIE 11797, Plasmonics: Design, Materials, Fabrication, Characterization, and Applications XIX, 117970E (1 August 2021); doi: 10.1117/12.2594110

SPIE.

Event: SPIE Nanoscience + Engineering, 2021, San Diego, California, United States

Multipolar scattering analysis of a hybrid metal-dielectric stacked nanoantenna

Andrei Kiselev*, Debdatta Ray, and Olivier J. F. Martin†
Nanophotonics and Metrology Laboratory, Swiss Federal Institute of Technology Lausanne (EPFL), 1015 Lausanne, Switzerland

ABSTRACT

Hybrid structures that combine dielectric resonators with plasmonic structures hold great promises due to the diversity of optical modes they possess. Here, we explore the physics underlying the scattering response of a hybrid nanoantenna made of a metal disk placed on top of a dielectric cylinder and study the hybridization of the different modes excited in the dielectric and metallic parts. Surprisingly, we note that the signature of an anapole state – usually only seen in high refractive index dielectrics – can be observed in the metallic part of the system. The Cartesian multipoles excited in the dielectric and metal interfere in a complex manner, leading to an unexpected high-order vector spherical multipolar response in the far-field. These effects are thoroughly studied in terms of the near-field and absorption enhancements. We also show that very fine control over the multipoles' resonant positions can be achieved by varying the geometry of the structure. This flexibility renders this system very promising for sensing applications. Based on these developments, we have designed and fabricated such hybrid nanoantennas using silicon and aluminum and measured a preliminary sensitivity of 160 nm/RIU, which is competing with conventional sensors based on localized surface plasmon resonances.

Keywords: Optical scattering, hybridization, plasmonics, sensing, nanofabrication

1. INTRODUCTION

Optical sensing at a desired wavelength has recently attracted significant interest. The techniques based on localized surface plasmon resonances have reported a sensitivity of hundreds of nm/RIU.[1,2] In these experiments, sensing of a refractive index variation is performed by tracking the variation of the scattered light resonance energy position. In this case, thanks to the resonant collective oscillations in metallic nanoparticles, an extremely high field enhancement can be reached, effectively increasing the sensitivity to the analytes' refractive index variations.[3] The sensitivity in these cases is determined by the quality factor of the resonances.

For a particular resonant particle geometry, that can take practically any shape such as spheres, stars, fractals, rods and many others, the form and the quality factor of the resonances mainly depends on the symmetry and sharpness of the edges of the structure and less on the sizes of the objects.[4-9] This is, however, not the case when several resonant particles are brought about in a close proximity to each other.[10,11] For two metal particles, the hybridization takes place leading to the emergence of additional high-quality factor resonances. However, as soon as the overall amount of metal is increased, so do also increase the losses, especially at the resonance frequencies. Quite interestingly, when hybridization is performed between metal and dielectric, the situation is expected to change. Low losses of dielectric should decrease the overall absorption of a hybrid system, whereas the magnetic type resonances should contribute to the resonant scattering characteristics, making the scattering response of the system more versatile. Indeed, in recent publications, the ability to manipulate the positions of the scattered field resonances has been shown on an example of a silver disk stacked on top of a silicon cylinder.[12] These developments helped designing and experimentally realizing an optimized structure with very high quality factor scattered field resonances that showed sensing at a level of 200 nm/RIU.[13]

In this paper, we make a comprehensive complementary work to Refs. [12,13] and analyze the hybridization effects in a similar geometry of stacked silicon-silver cylindric geometry in terms of the additional scattering peaks appearance, near-field and absorption enhancements.

*andrei.kiselev@epfl.ch,†olivier.martin@epfl.ch

Plasmonics: Design, Materials, Fabrication, Characterization, and Applications XIX, edited by Din Ping Tsai, Takuo Tanaka, Yu-Jung Lu, Proc. of SPIE Vol. 11797, 117970E · © 2021 SPIE
CCC code: 0277-786X/21/$21 · doi: 10.1117/12.2594110

2. RESULTS

In this section, we study the scattering response of a hybrid system made of an Ag disk placed on top of a Si cylinder as sketched in Figure 1(a). The Ag disk and Si cylinder share the same radius of 235 nm, with the heights of 24 and 88 nm, respectively. We model the refractive index of Ag with the experimental data fit obtained from Johnson and Christy[14] and the refractive index of Si was set as $\sqrt{13}$ without losses. A Si cylinder is chosen to be lossless to clearly estimate the absorption enhancement of a hybrid structure as compared to an isolated Ag disk, as shall be seen below. The hybrid system is illuminated with a planewave propagating along the symmetry axis of the structure, as depicted in Figure 1(a). For a hybrid structure, the total scattering cross section along with its vector spherical harmonic (VSH) contributions[15,16] is presented in Figure 1(a). Form Figure 1 (a), two distinct electric dipolar resonant peaks (E1) are observed at 980 and 1100 nm. Two scattering minima are observed at 850 and 1087 nm and marked with dashed grey vertical lines. To understand the origin of these resonant features, we plot the scattering cross sections of isolated Si cylinder and Ag disk in Figure 1(b) and 1(c), respectively. The illumination condition for these plots is kept the same as in Figure 1(a).

For a Si cylinder, Figure 1(b), we observe a strong electric dipolar resonance at 1060 nm and observe a part of a curve associated with the higher-energy dipolar resonance located at 760 nm. The resonance dip at 940 nm is attributed to the anapole state effectively excited in Si.[17,18] The scattering cross section of an isolated Ag disk, Figure 1(c), has only one electric dipolar resonance at 1250 nm within the chosen frequency range.

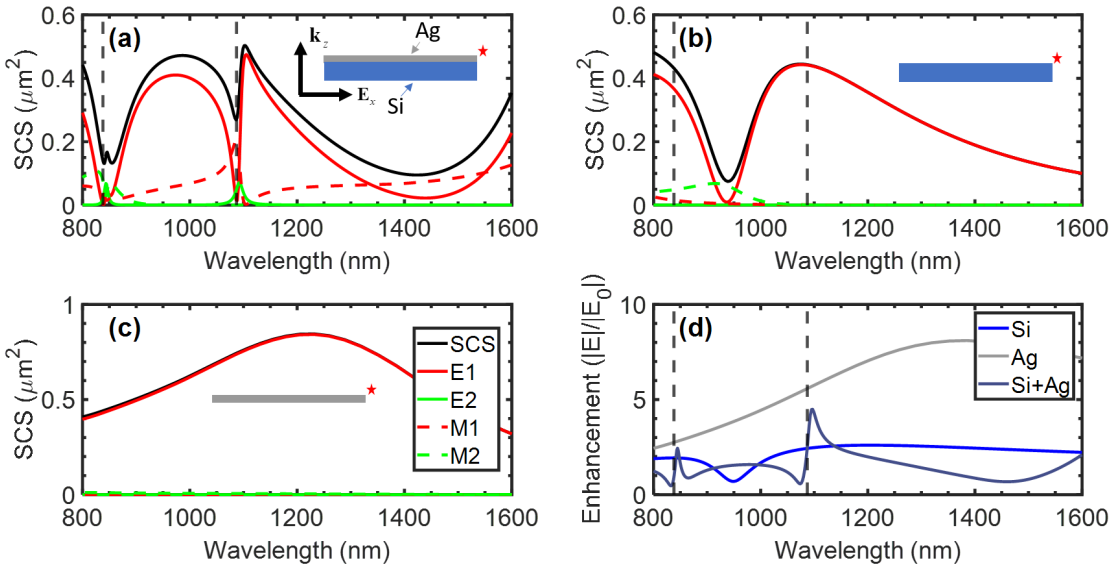

Figure 1. The scattering cross section with the VSH multipolar decomposition for (a) hybrid geometry of stacked Ag disk and Si cylinder (b) an isolated Si cylinder with a radius of 235 nm and a height of 88 nm, (c) an isolated Ag disk with a radius of 235 nm and a height of 24 nm. (d) Field enhancement at a point marked with a red star (located in the xOz-plane, 7 nm from the right top edge of the structure).

By comparing Figure 1(a)-1(c), we observe that the scattering of a hybrid geometry mainly inherits the scattering cross section line shape from a Si cylinder. The anapole state in a hybrid structure experiences a blueshift as compared to the position of the anapole state in Si. The electric dipole mode seen at 1060 nm for a Si structure is split into two modes at 980 and 1100 nm for a hybrid structure forming a Fano resonance.[6] This happens because the dipole mode at 1060 nm in Si effectively couples with the dipole mode in Ag at 1250 nm. This can be verified further by inspecting the charge distribution of Si and of a hybrid structure at 1050 and 1200 nm (below and above the position of the dipolar resonance in Si), Figure 2(a) and (b). We plot the charge distribution of isolated Si in Figure 2(a) and Figure 2(b), where it can be clearly seen that isolated Si shows the same charge distribution for the two selected wavelengths, whilst a hybrid structure clearly possesses two distinct resonance charge distributions, Figure 2(c) and Figure 2(d).

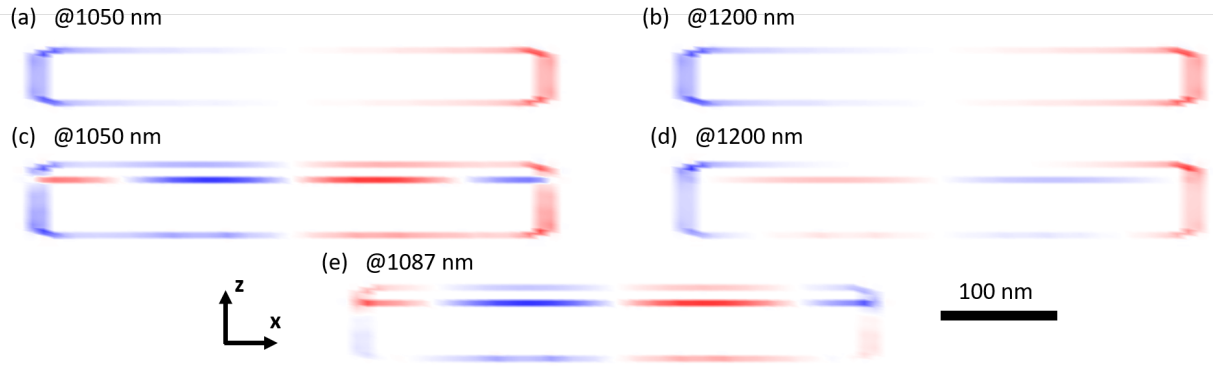

Figure 2. Real part of the normalized bound charge distribution. Red color stands for positive charges and blue for negative. (a) and (b) charge distributions for isolated Si cylinder at 1050 nm and 1200 nm. (c-e) charge distributions for a hybrid geometry at 1050 nm, 1200 nm and 1087 nm, respectively.

As can be noted from Figure 1(a), the scattering cross section of a hybrid geometry has a very sharp SCS resonance dip at 1087 nm. In the same time, we observe an effective enhancement of the magnetic dipole (M1) and electric quadrupole (E2) modes at this wavelength. In Figure 2(e) we plot the surface charge distribution for this resonant frequency that clearly points to an effective excitation of a resonant mode at this wavelength. It can be clearly noted that the phase of the charge on the Si and Ag parts of the hybrid structure are shifted by a factor of π, that is predicted by Fano resonance models.[6] Since the quality factor of the resonance at 1087 nm is very high, a significant field enhancement is expected at this wavelength. In Figure 1(e), we plot the field enhancement factor for isolated Si, Ag and a hybrid structure at a point that is located in the xOz plane at 7 nm from top right corner of the structure. It can be noted that for a hybrid system, the field enhancement is effectively lower as compared to that of Ag but higher than of Si. Hovewer, in the case of a hybrid system the enhancement is achieved at very particular wavelengths: at 850 and 1087 nm we see very distinct field enhancements.

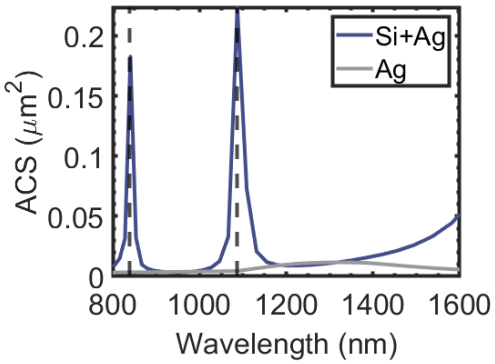

Figure 3. Absorption scattering cross sections of isolated silver disk (grey line) and of a hybrid system (dark blue).

Let us now analyze how dielectric affects losses in a hybrid system. In Figure 3, we plot the absorption scattering cross section for an isolated Ag disk and for a hybrid geometry (Si is not plotted as being lossless). It can be clearly seen that losses are significantly enhanced (about 50 times stronger) for a hybrid system at the position of the resonances. This can be explained by a penetration of strong volumetric electric fields from the dielectric structure into the metallic one, thanks to the continuity of the tangential component of the electric field across the boundary. Indeed, from Figure 4, we notice that for a hybrid system excited at 850 nm, the characteristic divergence-free field distribution of the anapole mode (that is usually seen in dielectric) can now be observed in metal.

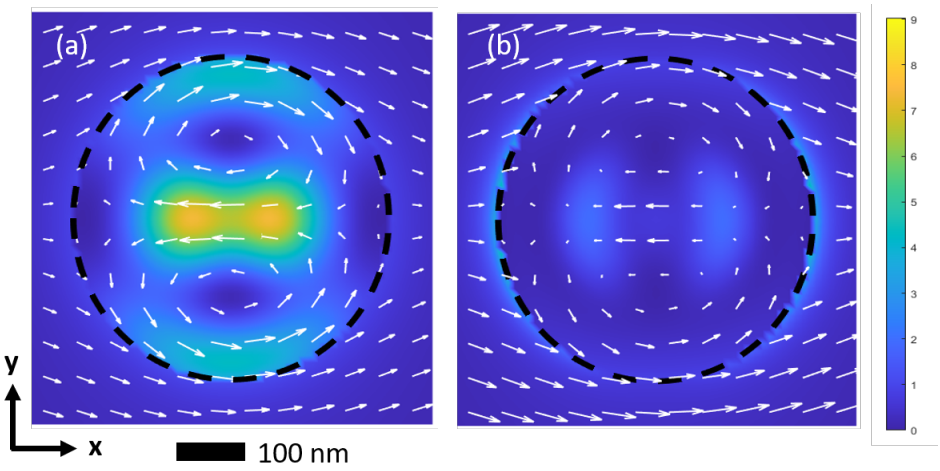

Figure 4. Electric field distribution (vectors) and intensity colormap. (a) At the geometrical center of a Si cylinder. (b) At the geometrical center of an Ag cylinder.

Quite interestingly, the positions and the magnitudes of the resonant features presented above can be finely controlled by varying the geometrical parameters of the structure. The analysis of the link between the magnitude/position of the individual multipolar components of the structure and geometrical parameters has been done in our recent work.[12] We would like to summarize its main results here. Let us call the height of the Si cylinder "H" and its radius "R". Let us also call the thickness of the Ag disk "t". In this case, we note that an increment of either R or H (or simultaneous increment of R & H) generally leads to an increment of the amplitude of the electric and magnetic dipole resonances with a simultaneous redshift of the resonance positions.[12] The increment of the height t of Ag, on the contrary, leads to a blueshift of the resonant positions and barely affects their amplitude, also leading to the emergence of high-quality resonances observed previously.[12]

The knowledge about these behaviors is very beneficial and helps us optimize and fabricate larger resonant structures. The fabricated optimized system is a periodically repeated unit sell having the size of 670x670 nm^2. Each cell consists of a Si cylinder and an Al disk having a height of 220 nm and 60 nm, respectively and sharing the same radius of 235 nm, see Figure 5(a). In order to further enhance the electric field produced by the structure, we introduce an additional 75 nm SiO_2 gap between Si and Al. It has been recently shown that the introduction of such a gap barely affects the magnitude of the resonances, while significantly affecting their positions.[10,12] Aluminum was chosen as the metallic component of a fabricated hybrid system instead of silver to ease the fabrication process. Moreover, the use of Al and Si makes the structure CMOS compatible.

We measure the transmittance spectrum of a designed structure suspended in air and in a glucose solution of varying concentration, corresponding to different refractive indices, Figure 5(b). See Ref.[12] for the technical details of the experiment. In Figure 5(b), we track the redshift of the resonant peak as the refractive index of the solution increases. By interpolating this dependence with linear regression, we estimate a preliminary accuracy of sensing at a level of 160 nm/RIU.

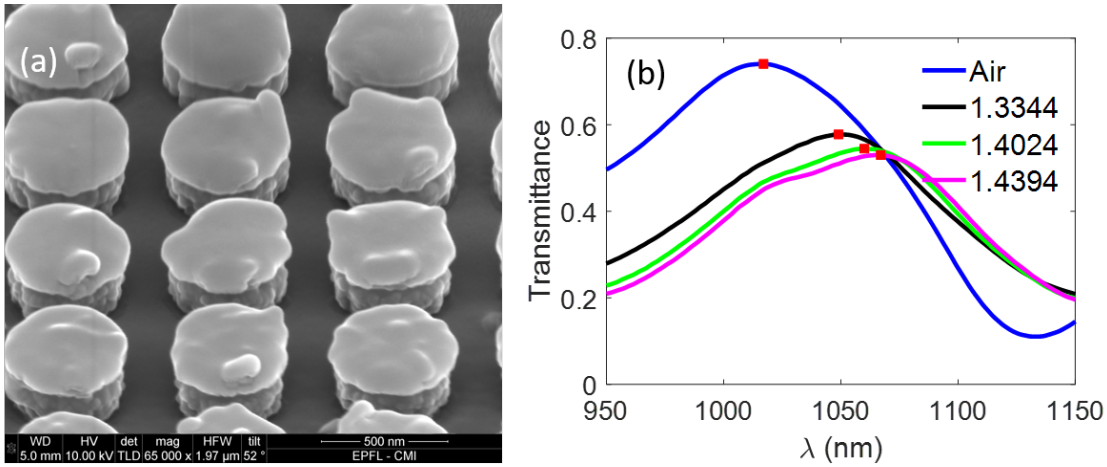

Figure 5. (a) SEM image of the fabricated structure. (b) Transmittance spectra of the designed structure performed in various environment.

3. CONCLUSIONS

We performed theoretical and experimental analysis of a hybrid structure made of a metal disk placed on top of a dielectric cylinder. Theoretical analysis revealed sharp multipolar resonance dips in the scattering spectrum of the hybrid structure appearing due to the emergence of the Fano resonance. In comparison between isolated metallic/dielectric parts and a hybrid structure, the latter shows very sharp resonance peaks, leading to strong field enhancements at particular wavelengths. In the meantime, ohmic losses are found to be increased by a factor of 50 at the same wavelengths.

A hybrid structure with additional spacing between metal and dielectric was fabricated and tested for sensing applications. Preliminary sensing at a level of 160 nm/RIU was detected.

ACKNOWLEDGMENTS

Funding from the European Research Council (ERC-2015-AdG-695206) and from the Swiss National Science Foundation (project 200021-162453) are gratefully acknowledged.

REFERENCES

1. M. Vala, S. Etheridge, J. A. Roach, and J. Homola, "Long-range surface plasmons for sensitive detection of bacterial analytes," Sensors and Actuators B: Chemical **139**(1), 59-63 (2009).
2. B. Špačková, P. Wrobel, M. Bocková, and J. Homola, "Optical Biosensors Based on Plasmonic Nanostructures: A Review," Proceedings of the IEEE **104**(12), 2380-2408 (2016).
3. S. A. Maier, *Plasmonics: fundamentals and applications* (Springer Science & Business Media, 2007).
4. E. P. Bellido, G. D. Bernasconi, D. Rossouw, J. r. m. Butet, O. J. Martin, and G. A. Botton, "Self-similarity of plasmon edge modes on Koch fractal antennas," ACS nano **11**(11), 11240-11249 (2017).
5. J. P. Kottmann, O. J. F. Martin, D. R. Smith, and S. Schultz, "Field polarization and polarization charge distributions in plasmon resonant nanoparticles," New Journal of Physics **2**27-27 (2000).
6. A. Lovera, B. Gallinet, P. Nordlander, and O. J. F. Martin, "Mechanisms of Fano Resonances in Coupled Plasmonic Systems," ACS Nano **7**(5), 4527-4536 (2013).
7. K. Achouri, A. Kiselev, and O. J. F. Martin, "Multipolar origin of electromagnetic transverse force resulting from two-wave interference," Phys. Rev. B **102**(8), 085107 (2020).
8. A. Kiselev, G. Bernasconi, and O. J. F. Martin, *Modes interplay controls the second harmonic generation dynamics of plasmonic nanostructures*, SPIE Nanoscience + Engineering (SPIE, 2020), Vol. 11462.

9. A. Kiselev, G. D. Bernasconi, and O. J. F. Martin, "Modes interplay and dynamics in the second harmonic generation of plasmonic nanostructures," Opt. Express **27**(26), 38708-38720 (2019).
10. Y. Ekinci, A. Christ, M. Agio, O. J. F. Martin, H. H. Solak, and J. F. Löffler, "Electric and magnetic resonances in arrays of coupled gold nanoparticle in-tandem pairs," Opt. Express **16**(17), 13287-13295 (2008).
11. J. Kim and O. J. F. Martin, "Studying the different coupling regimes for a plasmonic particle in a plasmonic trap," Opt. Express **27**(26), 38670-38682 (2019).
12. D. Ray, A. Kiselev, and O. J. Martin, "Multipolar scattering analysis of hybrid metal-dielectric nanostructures," arXiv preprint arXiv:2105.00670 (2021).
13. D. Ray, T. V. Raziman, C. Santschi, D. Etezadi, H. Altug, and O. J. F. Martin, "Hybrid Metal-Dielectric Metasurfaces for Refractive Index Sensing," Nano Lett. **20**(12), 8752-8759 (2020).
14. P. B. Johnson and R. W. Christy, "Optical Constants of the Noble Metals," Physical Review B **6**(12), 4370-4379 (1972).
15. S. Mühlig, C. Menzel, C. Rockstuhl, and F. Lederer, "Multipole analysis of meta-atoms," Metamaterials **5**(2), 64-73 (2011).
16. A. Kiselev, K. Achouri, and O. J. F. Martin, "Multipole interplay controls optical forces and ultra-directional scattering," Opt. Express **28**(19), 27547-27560 (2020).
17. F. Monticone, D. Sounas, A. Krasnok, and A. Alù, "Can a Nonradiating Mode Be Externally Excited? Nonscattering States versus Embedded Eigenstates," ACS Photonics **6**(12), 3108-3114 (2019).
18. E. A. Gurvitz, K. S. Ladutenko, P. A. Dergachev, A. B. Evlyukhin, A. E. Miroshnichenko, and A. S. Shalin, "The High-Order Toroidal Moments and Anapole States in All-Dielectric Photonics," Laser Photonics Rev. **13**(5), 1800266 (2019).